Study of the Magnetization Method Suitable for Fractional-Slot Concentrated-Winding Variable Magnetomotive-Force Memory Motor

Sari Maekawa, Kazuaki Yuki, Makoto Matsushita, Isamu Nitta, Yukihisa Hasegawa, Tsuyoshi Shiga, Tsuyoshi Hosoito, Kazunobu Nagai, and Hisao Kubota, *Member, IEEE*

***Abstract*—This paper describes a variable magnetomotive-force memory motor with a fractional-slot concentrated winding. We propose a method for optimal control of magnetization suitable for a fractional-slot concentrated winding. Our result shows that variable magnetized magnets are more highly magnetized when a fractional-slot concentrated winding is used than those using the conventional method.**

***Index Terms*—Current control, concentrated winding, fractional slot, magnetization, permanent-magnet synchronous motor (PMSM), variable magnetomotive-force memory motor.**

I. Introduction

GLOBAL warming has become a global problem. Therefore, we believe that the demand for energy-efficient motors, which are among the major sources of power consumption, will also increase in the future.

The permanent-magnet synchronous motor (PMSM) remains a relatively high-efficiency motor. The drive systems operate under a field-weakening mode in high-speed areas [1]–[3]. Therefore, the increase in copper loss is a major problem. Several techniques have been proposed, which dynamically change the magnitude of the magnetic field, to solve this problem. One of these techniques uses a variable magnetomotive-force memory motor (VMFM) [4], [5]. When a pulsed current flows through a coil, an armature reaction magnetic field is generated. When an external magnetic field is applied to the magnet by the magnetizing current, the magnetomotive force of the permanent magnet changes (see Fig. 1). The magnetic flux increases in proportion to the rotational speed. When the induced voltage becomes the upper limit of the supply voltage, the magnetomotive force of the permanent magnet decreases. As a result, both the magnetic flux and the induced voltage decrease.

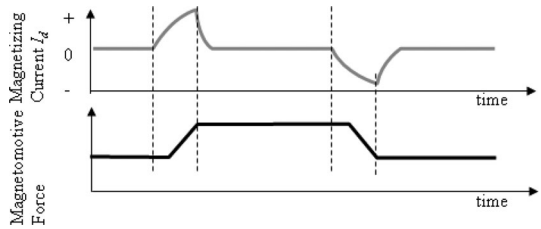

Fig. 1. Magnetizing current and magnetomotive force of the variable magnetized magnet.

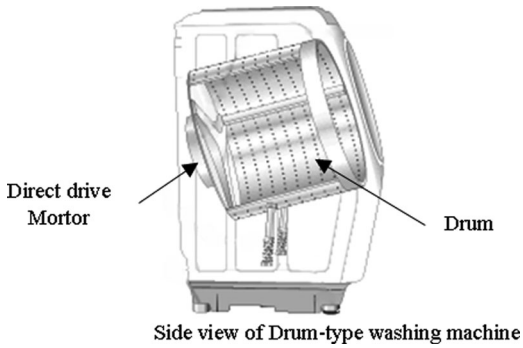

Fig. 2. Structure of a drum-type washing machine and the drive motor.

A concentrated-winding motor is often designed to improve power density and manufacturability [6]–[12]. The concentrated winding can shorten the coil end; thus, copper loss is reduced. Further, the motor will become smaller than the distributed-winding motor. Fig. 2 shows that the motors for washing machines is thin. The load characteristics of a washing-machine motor are shown in Fig. 3. The load areas for washing and drying are clearly designated, and these two areas account for a large portion of the motor load.

Generally, in a two-layer winding, the winding factor is low in a structure where three slots are present in one pole. The problem is that the core is likely to reach magnetic saturation as compared with that in the distributed winding. To solve this problem, a fractional-slot concentrated-winding motor is proposed where the number of slots per pole is fractional.

Manuscript received May 10, 2013; revised July 8, 2013, September 2, 2013, and October 20, 2013; accepted October 22, 2013. Date of current version April 30, 2014. Recommended for publication by Associate Editor J. O. Ojo.

S. Maekawa, K. Yuki, and M. Matsushita are with the Toshiba Corporation FUCHU Operations Power and Industrial Systems R&D Center 1, Toshiba-Cho, Fuchu-Shi, Tokyo 183-8511, Japan (e-mail: sari1.maekawa@toshiba.co.jp; kazuaki.yuki@toshiba.co.jp; makoto.matsushita@toshiba.co.jp).

I. Nitta and Y. Hasegawa are with the Toshiba Corporation Yokohama Complex 33, Shin-Isogo-Cho, Isogo-Ku,Yokohama-Shi, Kanagawa 235-0017, Japan (e-mail:sam.nitta@toshiba.co.jp; yukihisa.hasegawa@toshiba.co.jp).

T. Shiga, T. Hosoito, and K. Nagai are with the Toshiba Home Appliances Corporation 991, Anada-Cho, Seto-Shi, Aichi, Aichi 489-8610, Japan (e-mail: tsuyoshi.shiga@toshiba.co.jp; tsuyoshi.hosoito@glb.toshiba.co.jp; jumbo.nagai@toshiba.co.jp).

H. Kubota is with the Meiji University School of Science and Technology, 1-1-1, Higashi-mita, Tama-ku, Kawasaki 214-8571, Japan (e-mail: kubota@isc.meiji.ac.jp).

Color versions of one or more of the figures in this paper are available online at http://ieeexplore.ieee.org.

Digital Object Identifier 10.1109/TPEL.2013.2288635

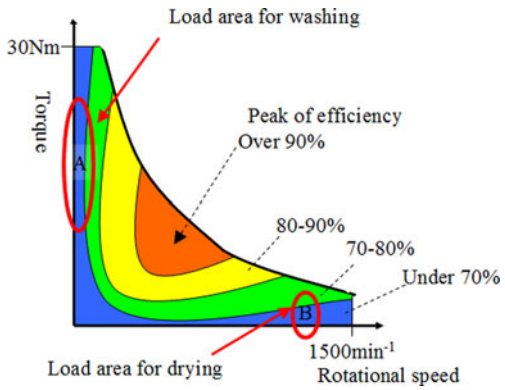

Fig. 3. Load areas of the washing machine for washing and drying are clearly divided.

VMFMs have been studied for distributed winding, taking into consideration the effects of magnetic saturation [13]–[17]. However, the magnetization method and magnetization characteristics of variable magnetized magnets that are used for a fractional-slot concentrated winding have not been clarified in detail until now [18], [19].

This study examines the following three points regarding a VMFM with a fractional-slot concentrated winding:

1) difference in the magnetization characteristics of the slot combination;
2) magnetization control method suitable for fractional-slot concentrated-winding motors;
3) quantitative comparison of the 24-pole/36-slot and 48-pole/36-slot motors.

The 24-pole/36-slot configuration is chosen as the slot combination for a general concentrated winding. In contrast, the 48-pole/36-slot configuration is chosen as the model for effectively magnetizing a variable magnetized magnet.

II. Principle of Variable Magnetomotive-Force Motor

A. Permanent Magnet for Variable Magnetomotive Force

A permanent magnet has a large coercive force and generates magnetic flux throughout the magnetic circuit. The magnetomotive force of a permanent magnet can be varied by an external magnetic field. To accomplish this task, a large magnetic field is required, which must be larger than the coercive force of the permanent magnet. However, the external magnetic field generated by magnetizing current I_d is limited by the rating of the inverter. In addition, when the coercive force H_{cj} is very small, the magnetic force of the variable magnetized magnets is changed by the load current I_q. Consequently, H_{cj} of the variable magnetized magnet is approximately 100–400 kA/m and can be suited for this purpose.

The specification of the magnets used for the proposed design is shown in Table I and Fig. 4. The Nd–Fe–B grade is 42B. Sm–Co magnets are chosen as variable magnetized magnets because they have low H_{cj} and high magnetic flux density B_r. When an Al–Ni–Co magnet is used, the following problem arises. An object with high magnetic flux density has a very low coercive force ($H_{cj} < 100$ kA/m). When the coercive force is very low, the magnetomotive force of the magnet is changed by I_q. Because the magnetic flux density B_r is very low, a ferrite magnet cannot be used.

TABLE I
Specifications of the Magnet

Constant magnetized magnet (Nd-Fe-B, 42)	Residual magnetic flux density B_r	1.33T
	Coercive force H_{cj}	1000kA/m
	Operating temperature	20° C
Variable Magnetized magnet (Sm-Co, No Grade)	Residual magnetic flux density B_r	1.05T
	Coercive force H_{cj}	100~400kA/m
	Operating temperature	20° C

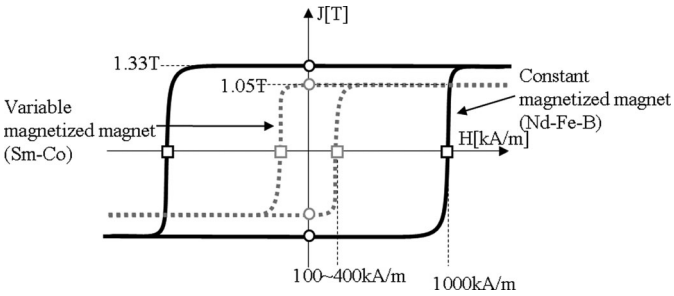

Fig. 4. Specifications of the magnet.

The Sm–Co magnet used as a variable magnetized magnet has an appropriate H_{cj} resulting from a special production method. This production method cannot be revealed here because it is a trade secret; thus, no general grading is available. The operating temperature for both Nd–Fe–B and Sm–Co magnets is at room temperature, i.e., 20 °C.

B. Principle of Variable Magnetomotive Force

We describe the change characteristics of the magnetization by the magnetizing current. Magnetization J is expressed in (1) in terms of the magnetic field H that acts on the magnet

$$J = B - \mu_0 H. \tag{1}$$

First, we describe the process of decreasing the magnetization. The magnet is magnetized at Point (1) for the initial state, as shown in Fig. 5(a), which shows the magnetic property curve in the high-speed and small-torque area, designated as point B in Fig. 3. The variable magnetized magnets are demagnetized under this operating condition. In this state, the inverter applies demagnetizing current $-I_d$ required to decrease the magnetization. As a result, an external magnetic field $-H$ is applied. Then, the magnetization is brought down to Point (2). The motor operates in the demagnetized state. Because the external magnetic field H generated by I_q is smaller than H_{cj}, magnetization of the variable magnetized magnet is maintained under the state of decreasing magnetization, as shown in Fig. 5(a). Because the induced voltage decreases owing to the decreasing magnetization, the field-weakening current decreases compared with that in the conventional PMSM. Moreover, the iron loss also decreases. The efficiency in the high-speed area is improved by these processes.

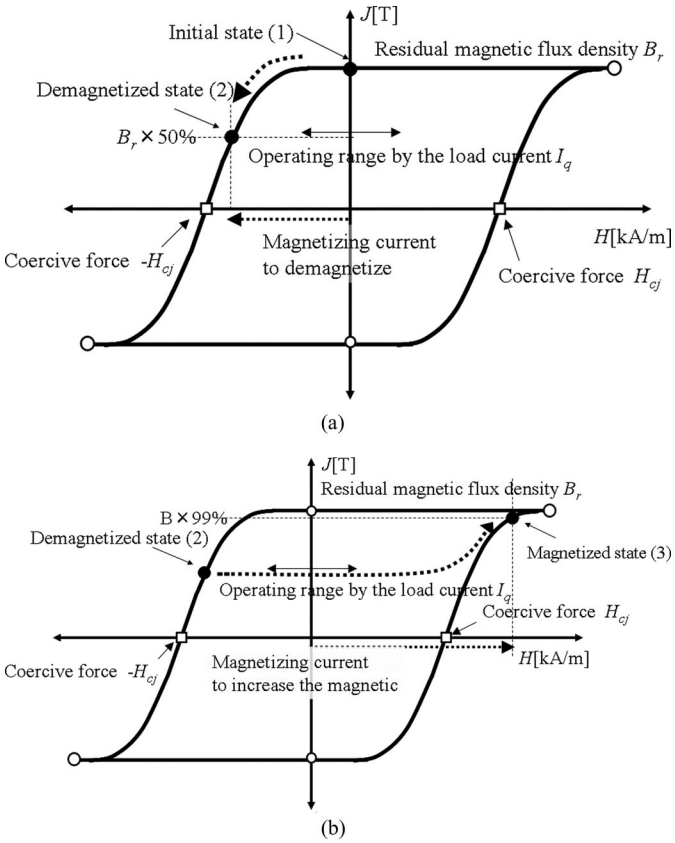

Fig. 5. Magnetic property curve of the variable magnetized magnet. (a) Decreasing magnetization. (b) Increasing magnetization.

Fig. 5(b) shows the magnetic property curve in the low-speed area, shown as point A in Fig. 3. We now describe the process of increasing magnetization. The state of magnetization is at Point (2) after the decreasing magnetization, as shown in Fig. 5(b). During this state, the inverter applies external magnetic field $+H$, generated by magnetizing current $+I_d$, required to increase the magnetization. The variable magnetized magnet is magnetized to Point (3). As a result, the magnetomotive force increases and generates a large torque.

When the rotation speed changes, the magnetomotive force of the variable magnet is changed to a suitable value, as shown Fig. 5(a) and (b). Therefore, the efficiency is improved under various operating conditions.

C. Structure of the Variable Magnetomotive-Force Motor

The VMFM configuration is shown in Fig. 6. The rotor is a combination of a high-coercivity magnet (constant magnetized magnet) and a low-coercivity magnet (variable magnetized magnet). VMFM is classified into series and parallel magnetic circuits, as shown in Fig. 6 [3]

The series-type circuit is further classified into two types, as shown in Fig. 7. Fig. 7(a) shows two types of magnets placed in one pole. Fig. 7(b) shows one type of magnet in one pole. In this study, we design the VMFM similar to the type shown in Fig. 7(b).

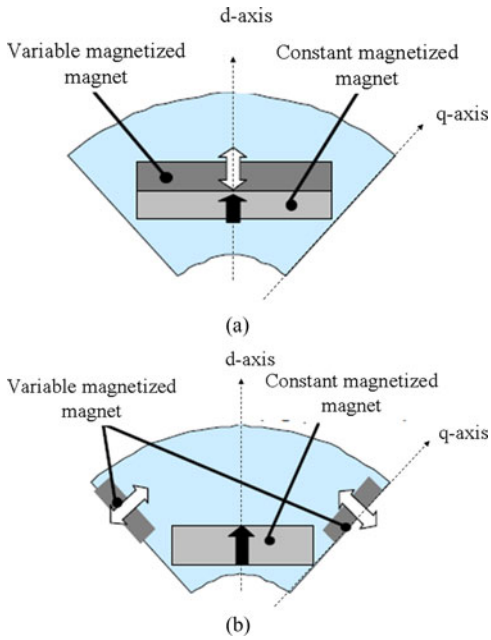

Fig. 6. Basic configuration of the VMFM. (a) Series magnetic circuit type. (b) Parallel magnetic circuit type.

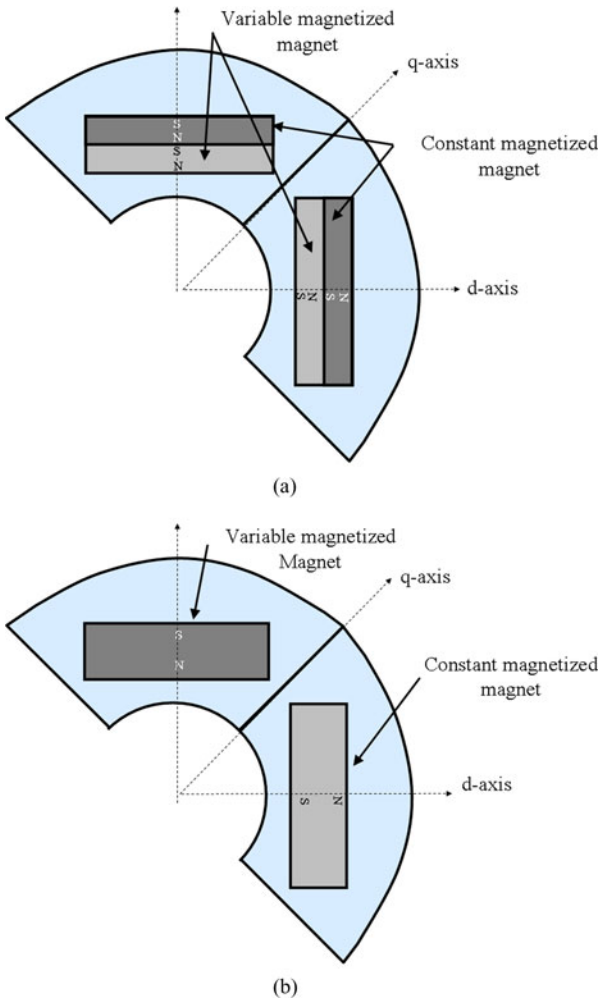

Fig. 7. Difference arising from the number of magnets. (a) Series type: two kinds of magnets in one pole. (b) Series type: one kind of magnet in one pole.

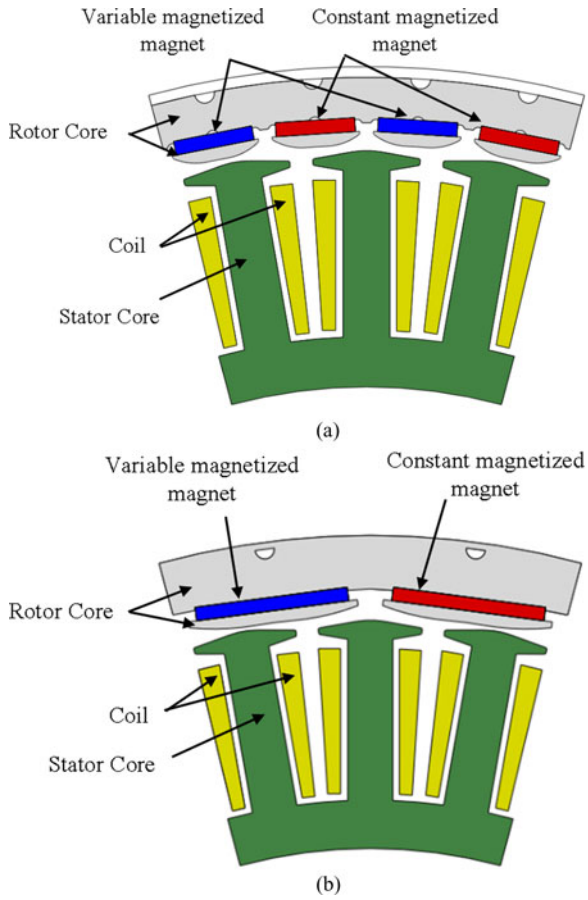

Fig. 8. Model of the fractional-slot concentrated-winding VMFM. (a) Actual cross sections of a 48-pole 36-slot motor. (b) Actual cross sections of a 24-pole 36-slot motor.

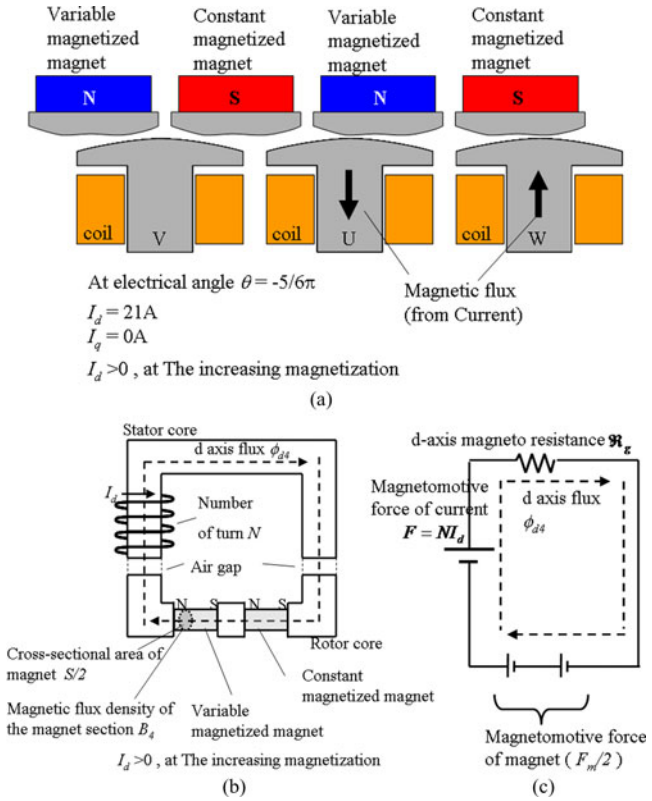

Fig. 9. Magnetization method of the four-pole/three-slot variable magnetic force concentrated-winding motor. (a) Current phase and magnetization angle. (b) Magnetic circuit models of magnetization. (c) Equivalent circuit.

III. Fractional-Slot Concentrated-Winding Motor

A. Verification Model of the Fractional-Slot Concentrated-Winding Motor

Fig. 8 shows a model of the fractional-slot concentrated-winding VMFM. Fig. 8(a) shows a 48-pole 36-slot motor, and Fig. 8(b) shows a 24-pole 36-slot motor. These motors are series-type VMFMs. The variable and constant magnetized magnets are alternately arranged in each pole. In the following, we consider the three-slot type. Therefore, the 48-pole 36-slot motor is referred to as a four-pole/three-slot motor, and the 24-pole 36-slot motor is referred to as a two-pole/three-slot motor.

In general, the four-pole/three-slot motor suffers from a problem in that the rotor loss (iron loss) is large in the high-speed area. However, the variable magnetized magnet is demagnetized in the high-speed area. As a result, the magnetic flux, as well as the iron loss, decreases. Therefore, the decreasing magnetization is important.

The magnetizing current of the series-type VMFM is less than that of the parallel-type VMFM. We describe the reason for this difference. In the series-type VMFM, the variable and constant magnetized magnets are arranged in series in the magnetic circuit. Therefore, the magnetic field in the forward direction is always applied to the variable magnetized magnet. As a result, the external magnetic field of the variable magnetized magnet owing to the magnetizing current is less than that in the parallel-type VMFM.

Furthermore, the lower limit of the variable magnet is restricted by the constant magnetized magnet. For example, even if the external magnetic field generated by the magnetizing current greatly reduces the magnetization of the variable magnetized magnet, the magnetization returns to a certain value owing to the magnetic field of the constant magnetized magnet.

B. Increase in Magnetic Field Due to the Action of Fractional-Slot Concentrated Winding

In the four-pole/three-slot and two-pole/three-slot motors, I_d flows in the directions shown in Figs. 9(a) and 10(a), respectively. The external magnetic field acting on the variable magnetized magnet is calculated by (2)–(8). Figs. 9(b) and (c) and 10(b) and (c) show the magnetic-circuit model at the time of flow of the magnetizing current

$$F = NI_d \tag{2}$$

$$\phi_{d2} = \frac{NI_d + F_m}{\Re_g} \tag{3}$$

$$B_2 = \frac{\phi_{d2}}{S} = \frac{NI_d + F_m}{\Re_g S} \tag{4}$$

$$H_2 = \frac{B}{\mu} = \frac{NI_d + F_m}{\mu \Re_g S} \tag{5}$$

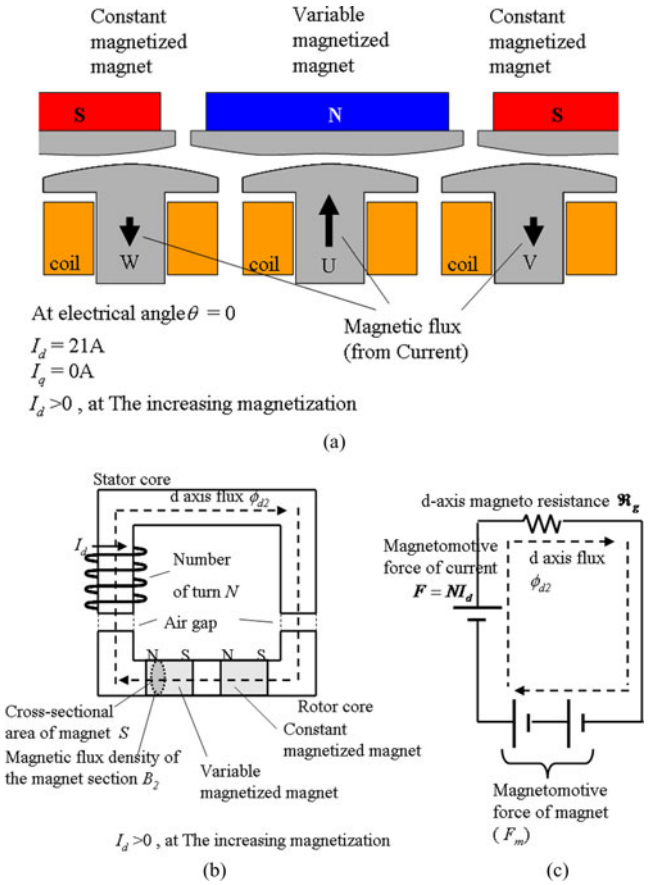

Fig. 10. Magnetization method of the two-pole/three-slot-variable magnetic force concentrated-winding motor. (a) Current phase and magnetization angle. (b) Magnetic circuit models of magnetization. (c) Equivalent circuit.

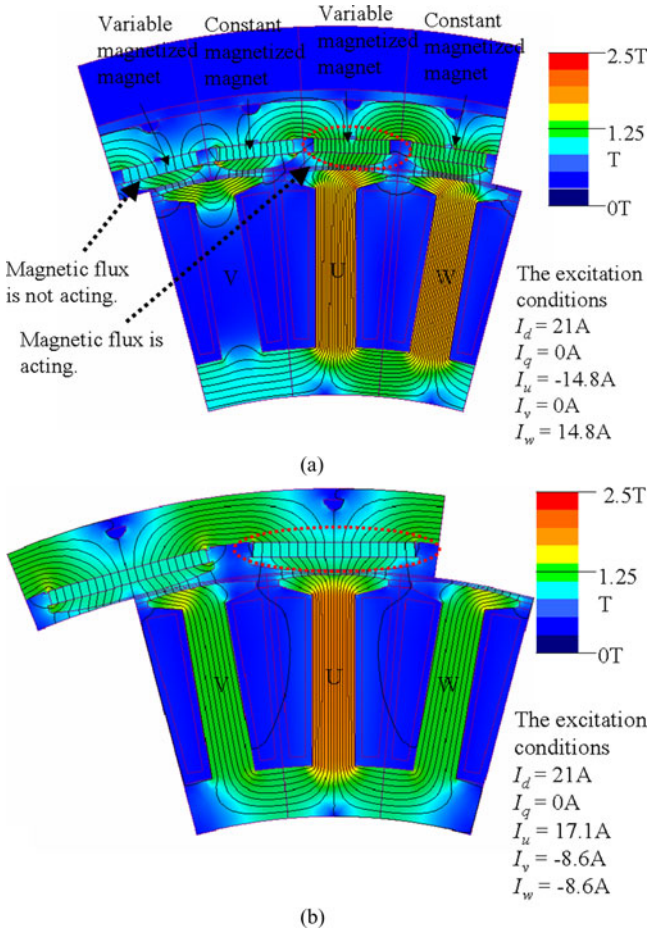

Fig. 11. Comparison of the magnetic flux density due to the differences in the slot configuration. (a) Four pole/three slot Motor. (b) Two pole/three slot motor.

$$\phi_{d4} = \frac{NI_d + \frac{F_m}{2}}{\Re_g} \tag{6}$$

$$B_4 = \frac{\phi_{d4}}{\frac{S}{2}} = \frac{2NI_d + F_m}{\Re_g S} \tag{7}$$

$$H_4 = \frac{B}{\mu} = \frac{2NI_d + F_m}{\mu \Re_g S} \tag{8}$$

where

F Winding magnetomotive force due to the magnetizing current (A).
N Number of turns.
I_d Magnetizing current (A).
Φ_{d2} d-axis flux (two-pole/three-slot) (Wb).
Φ_{d4} d-axis flux (four-pole/three-slot) (Wb).
F_m Magnetomotive force due to the permanent magnet (A).
R_g d-axis magnetoresistance (A/Wb).
S Cross-sectional area of the magnet (m^2).
B_2 Magnetic flux density inside the variable magnetized magnet (two-pole/three-slot) (T).
B_4 Magnetic flux density inside the variable magnetized magnet (four-pole/three-slot) (T).
H_2 External magnetic field (two-pole/three-slot) (T).
H_4 External magnetic field (four-pole/three-slot) (T).

The value of the current that flows in both types is the same, and the stator has the same shape. In (4) and (7), the cross-sectional area S of the magnet for the two-pole/three-slot motor is larger than that for the four-pole/three-slot motor. Therefore, the external magnetic field for the four-pole/three-slot motor is larger than that for the two-pole/three-slot, as shown in (5) and (8).

Fig. 11 shows the simulation results of the magnetic flux density B analyzed by FEM. The I_d values in Fig. 11(a) and (b) are the same ($I_d = 21$ A, $I_q = 0$ A, $I_u = 17.1$ A, $I_v = -8.6$ A, and $I_w = -8.6$ A), and the magnetic flux density B values of the stator in Fig. 11(a) and (b) are almost the same. In contrast, the magnetic flux density B in the variable magnetized magnet for the four-pole/three-slot motor is higher than that for the two-pole/three-slot motor. By using the four-poles/three-slot fractional-slot concentrated-winding configuration, the external magnetic field is applied effectively to the variable magnetized magnet.

Fig. 11(a) shows that the magnetic flux acts on the two right-hand side magnets but not on the left-hand side magnets. To magnetize all the magnets to the same extent, I_d must flow twice. This magnetization process is shown in Fig. 12(a)–(c).

First, the magnetizing current flows at the time when the electrical angle θ is $-5/6\pi$, as shown in Fig. 12(a). The current flows

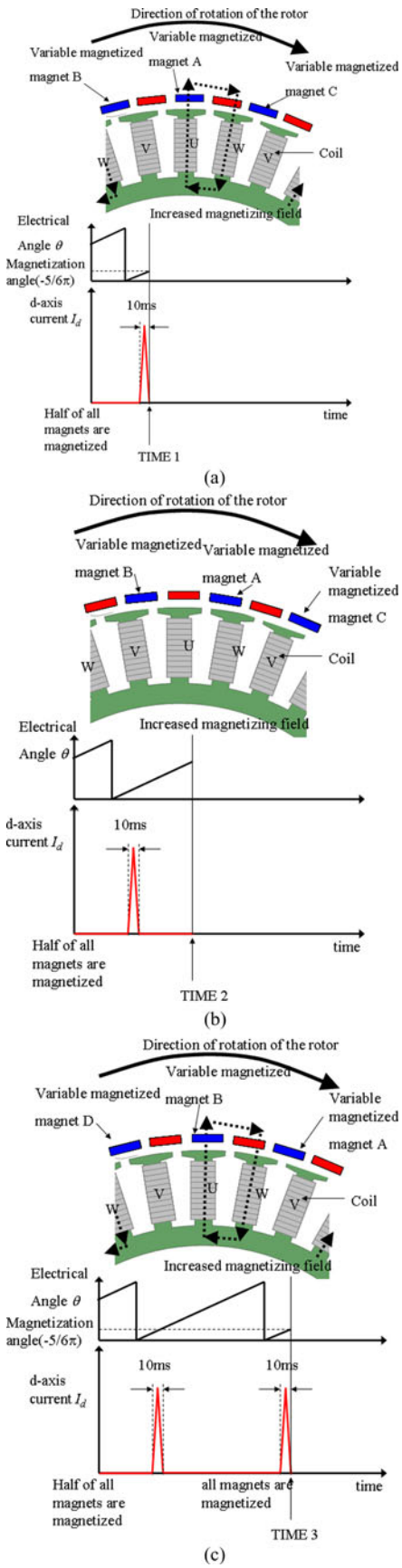

Fig. 12. Magnetization process (four-pole/three-slot motor). (a) First magnetization. (b) After first magnetization. (c) Second magnetization.

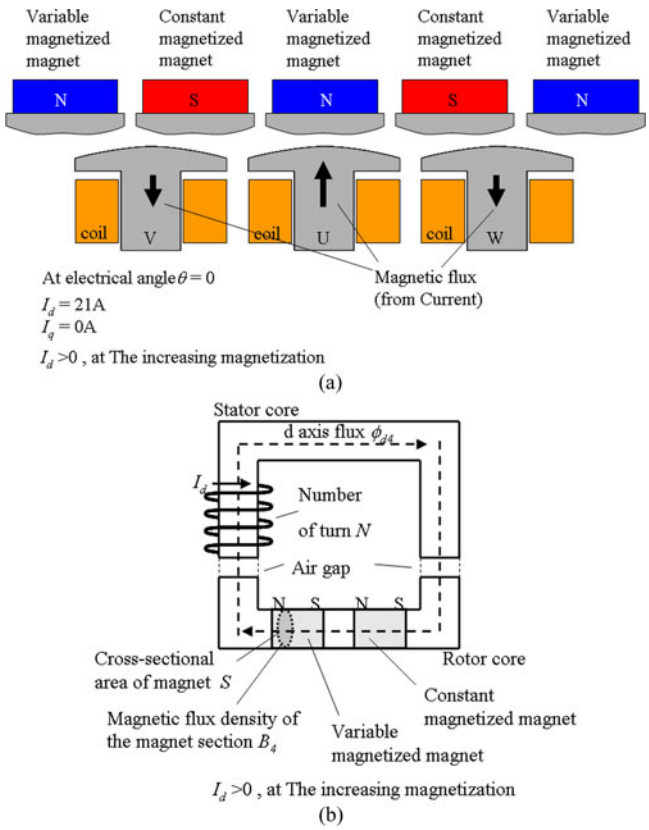

Fig. 13. All magnets are magnetized at the same time (four-pole/three-slot motor). The magnetization angle is not $5/6\pi(0°)$. (a) Current phase and magnetization angle. (b) Magnetic circuit models of magnetization.

only through the U and W phases. This current is I_d (>0). At this time (TIME1), variable magnetized magnet A is magnetized, and variable magnetized magnets B and C are not magnetized. Then, the rotor rotates [see Fig. 12(b)]. No magnetizing current flows at this instant (TIME2). The second magnetizing current flows when θ becomes the same as that shown in Fig. 12(a) [see Fig. 12(c)]. Variable magnetized magnet B is magnetized at this instant (TIME3). Although variable magnetized magnets A and D are not magnetized, they are already magnetized by the first magnetizing current.

All variable magnetized magnets are now magnetized to the same extent, and the magnetization process is complete.

If a fractional-slot concentrated winding is used, two or more magnetization processes are needed, as mentioned above. One of the reasons why we choose the four-pole/three-slot motor is that the number of magnetization is only two [see Fig. 12(a)–(c)]. When magnetization occurs frequently, product application becomes difficult.

C. Angular Dependence of the Magnetization Characteristic

At $\theta = -5/6\pi$ [see Fig. 9(a)], the d-axis magnetic flux caused by the magnetizing current passes through only two magnets, including the variable magnetized magnet. In contrast, the d-axis magnetic path is formed along the four magnets at the position shown in Fig. 13. When the electrical angle is not equal

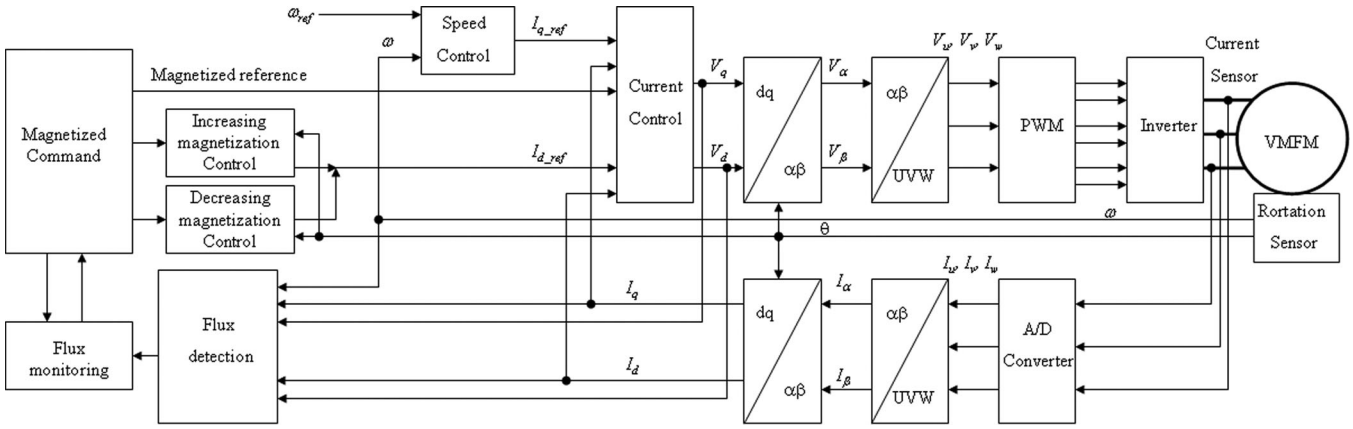

Fig. 14. Control configuration.

to $-5/6\pi$, the d-axis magnetic equivalent circuit is shown in Fig. 13. At this electrical angle ($\theta = 0$), the cross-sectional area of the variable magnetized magnets S increases twice than that for Fig. 9. Therefore, the external magnetic field H and the magnetic flux density B of the variable magnetized magnet are smaller than those at $\theta = -5/6\pi$. As a result, even if the magnetizing current flows, the magnetization of the variable magnetized magnet does not change, i.e., it is a failure. In other words, the magnetic circuit of a four-pole/three-slot motor has angle-dependent magnetic properties. The electrical angle for the smallest S at the time of magnetization is $-5/6\pi$. The effect of magnetization at this electrical angle is verified by the experimental result.

IV. Magnetization Control

Fig. 14 shows the configuration of the motor control and the control of the magnetizing current. To verify the proposed method, an IPMSM without saliency is used (explained later in Table II). Therefore, even if the torque of the motor is controlled by I_q and the magnetization is controlled by I_d, the torque ripple does not worsen. I_d flows twice at "the magnetization angle," which is $-5/6\pi$.

The external magnetic field H acts on the variable magnetized magnet for a short time, e.g., 10 ms. When I_d flows at an electrical angle different from "the magnetization angle," the variable magnetized magnet is not maximally magnetized. Furthermore, when the motor rotation is fast, the time for the electrical angle to be in "the magnetization angle" is very short. Therefore, the current control requires a high speed. Fig. 15 shows the configuration of the current control unit for high-speed control of I_d.

During the magnetization command, the magnetizing current command I_{d_ref} is converted into a d-axis voltage command value using the inverse motor model. In other words, the d-axis current I_d is controlled by a feed-forward (FF) voltage command during magnetization. Further, the q-axis current I_q is controlled by a feedback (FB) current command. The magnetization control is configured to be a combination of the two controls. After the magnetization control finishes, the d-axis current control returns to FB control. Using these controls, the proposed method realizes high-speed magnetizing current control and torque ripple control.

TABLE II
Key Design Data

Motor	Motor type	Variable Magnetomotive Force Memory Motor
	Magnetic circuit	Radial gap type
	diameter of the motor	ϕ252mm
	Stack length	40.9mm
	Total weight	4780g
	Saliency ratio(L_q/L_d)	1.05
	Maximum Speed	1500min^{-1}
	Rated Torque	30Nm
	Operating temperature	20℃
Stator	Configuration of the stator	Outward salient : 36slot
	Method of winding	Concentrated Winding
Rotor	Configuration of the rotor	Outer rotor
	Number of magnet	48pole (24 Pair)
	Fixing method of the magnet	IPM
Electrical Ratings	DC Voltage	280V
	Rated current of inverter	7Arms

V. Experiment

A. Characteristics of the Variable Magnetomotive Force

Figs. 16 and 17 show photographs of the VMFM to test. Figs. 16 and 17 show the rotor and stator, respectively. Table II shows the specifications of the test motor. This motor is an outer rotor type. Fig. 18 shows the variable characteristics of the induced voltage when I_d flows into the motor. When the magnetizing current flows, the induced voltage of the motor varies by approximately 20%. At this time, the magnetizing current is approximately 20 A (=3 p.u.).

Fig. 19 shows the comparison of the minimum and maximum magnetization characteristics of the two-pole/three-slot and four-pole/three-slot motors. In the four-pole/three-slot motor configuration, the maximum amount of induced voltage,

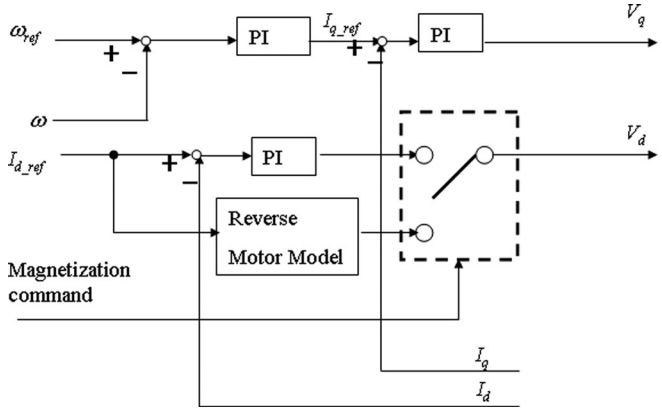

Fig. 15. Configuration of the current control.

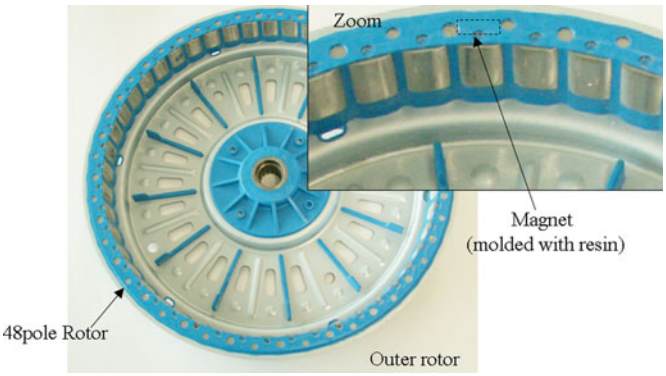

Fig. 16. Rotor of the VMFM used in the experiment (48 poles, 36 slots).

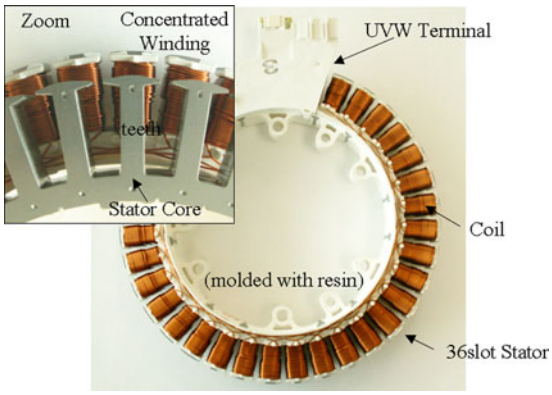

Fig. 17. Stator of the VMFM used in the experiment (48 poles, 36 slots).

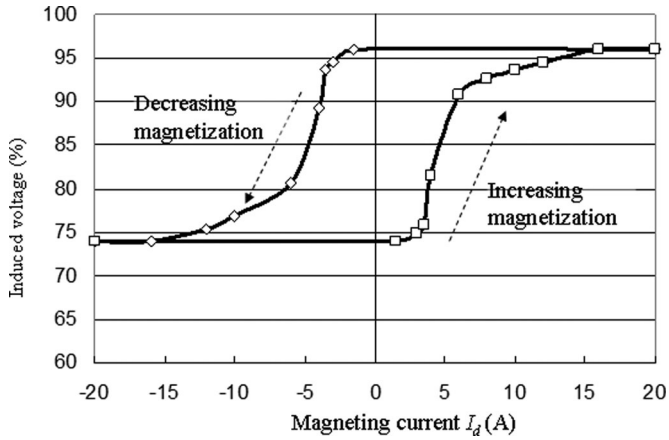

Fig. 18. Variable characteristics of the VMFM.

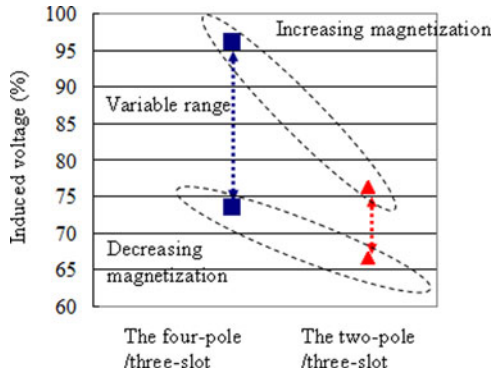

Fig. 19. Comparison of the magnetic force variable characteristic of the two-pole/three-slot and four-pole/three-slot motors.

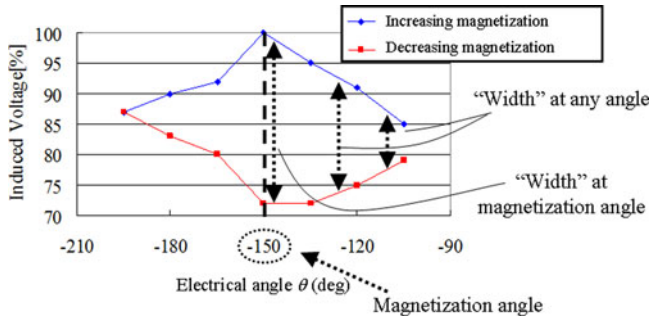

Fig. 20. Angular dependence of the magnetization characteristic.

as well as the range of the variable magnetomotive force increases.

Fig. 20 shows the magnetic properties when the electrical angle changes at the time of magnetization. When the variable magnetized magnet is magnetized at the "magnetization angle" ($\theta = -5/6\pi$), the induced voltage varies between the maximum and the minimum. At this electrical angle, the magnetic flux caused by the magnetizing current is applied to only two magnets, including the variable magnetized magnet. In contrast, when magnetization is done outside the "magnetization angle," the width, which represents the maximum and minimum differences, is reduced.

B. *Characteristics of the Two Times Magnetization*

Fig. 21 shows the experimental result of the induced voltage measured between the motor terminal and a neutral point. Current is not flowing. The motor is rotated by external force. Fig. 21(a) shows the waveform of the induced voltage of the four-pole/three-slot motor when magnetized only once. The amplitude of the induced voltage in each pole is different, which means that only half of all the variable magnetized magnets are magnetized. When the motor is magnetized twice, all poles are at the same magnetization level, as shown in Fig. 21(b), and the amplitude of the induced voltage becomes constant. The result

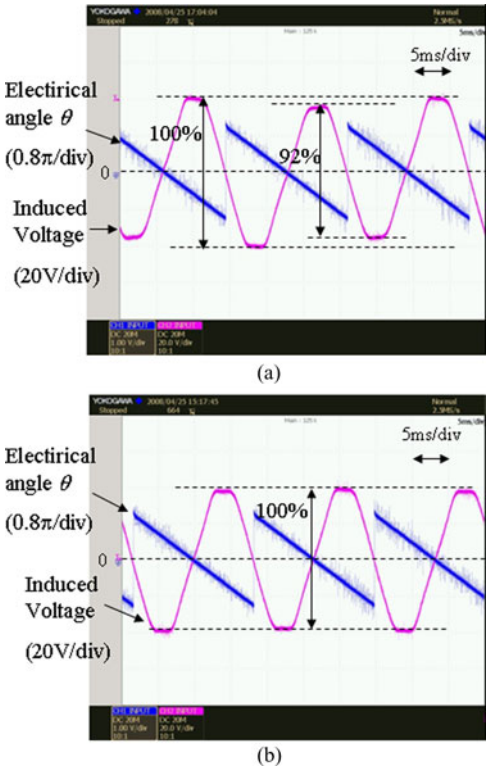

Fig. 21. Induced voltage waveform after magnetization.

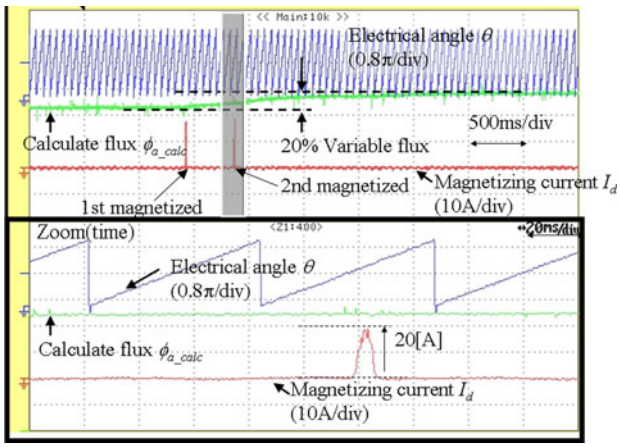

Fig. 22. Control characteristics of the magnetizing current.

shows the importance of the two times flow of the magnetizing current.

C. Control Characteristics of the Magnetizing Current

Fig. 22 shows the characteristics of the current control at the time of magnetization. I_d flows for approximately 10 ms under FF and FB current controls. After the magnetizing current flows, the calculated flux ϕ_{a_calc} increases, as shown in Fig. 22. Because the induced voltage cannot be measured by the same method shown in Fig. 21 during the current flow, ϕ_{a_calc} is calculated by (9)

$$\phi_{a\_calc} = \frac{V_q - RI_q - \omega L_d I_d}{\omega} \tag{9}$$

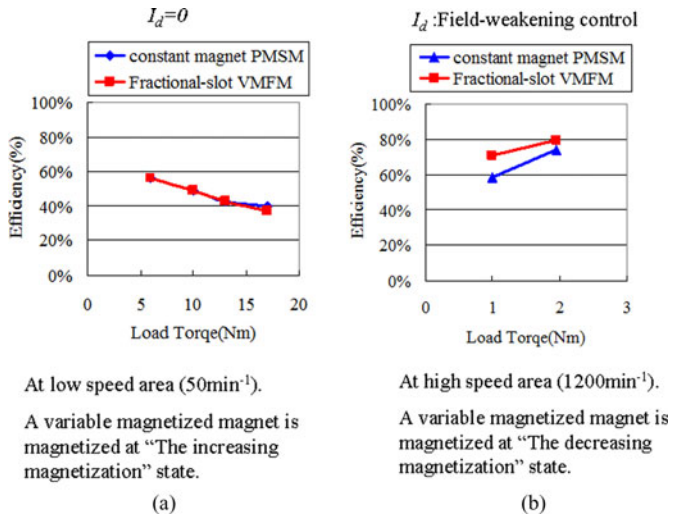

Fig. 23. Efficiency improvement of the VMFM. (a) Low-speed area (point A). (b) High-speed area (point B).

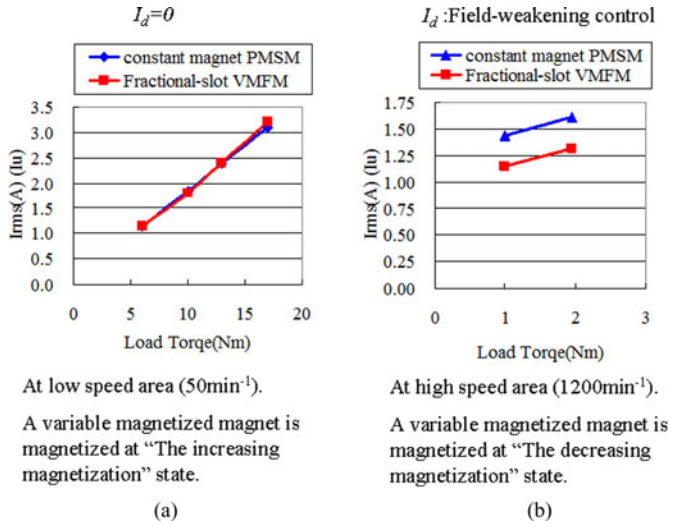

Fig. 24. Reduction in current $I_{\rm rms}$ of the VMFM. (a) Low-speed area (point A). (b) High-speed area (point B).

where

ϕ_{a_calc}	Calculated motor flux (Wb).
V_q	q-axis voltage (V).
I_d	d-axis current (A).
I_q	q-axis current (A).
R	Winding resistance (A).
L_d	q-axis inductance (A).
ω	Rotation speed of the motor (rad/s).

D. Result of Improved Efficiency

Fig. 23(a) and (b) shows the comparison of the efficiency characteristics of the fractional-slot concentrated-winding VMFM and the conventional PMSM. The compared points are the main load areas of the washing machine shown in Fig. 3. Fig. 25 shows the load points of the washing and drying areas. Fig. 23(a) shows the efficiency characteristics in the low-speed area (50 $\rm min^{-1}$), which is indicated by A in Fig. 25. Fig. 23(b) shows the

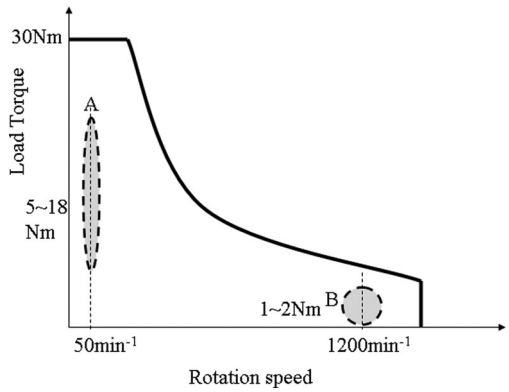

Fig. 25. Load area used in the efficiency evaluation.

efficiency characteristics of the high-speed area (1200 min^{-1}), which is indicated by B in Fig. 25. The efficiency is improved by reducing the magnetic force at 1200 min^{-1}. The reason for the improvement in the efficiency at the high-speed area is that the field-weakening current is decreased by the decreasing magnetization.

Fig. 24(a) and (b) shows the comparison of current I_{rms}. At the low-speed area, since VMFM operates in the increasing magnetization state (96% induced voltage shown in Fig. 18), the current I_{rms} is equivalent to that for PMSM. In contrast, at the high-speed area, the field-weakening current is decreased by the decreasing magnetization (75% induced voltage shown in Fig. 18).

VI. Conclusion

We have investigated the magnetization of a VMFM with a fractional-slot concentrated winding and obtained the following conclusions:

1) At the magnetization state, the variable magnetized magnet was magnetized to a higher magnetic flux density using the fractional-slot concentrated-winding configuration of the four-pole/three-slot motor.
2) Only half of the variable magnetized magnets were magnetized in the first magnetization, and the other magnets were magnetized in the second magnetization. When I_d flowed at a specific electrical angle ($-5/6\pi$), the external magnetic field H effectively magnetized the variable magnetized magnet. I_d was controlled by the combination of the FB current control and the FF voltage control. A high-speed magnetizing current control was realized.
3) We used the two-pole/three-slot and four-pole/three-slot motors as examples. We quantitatively compared their magnetic properties.

As a result, the proposed method enables the realization of highly efficient characteristics. In the future, we will examine the other optimal fractional-slot configurations of VMFMs.

References

[1] T. Jahns, "Flux-weakening regime operation of an interior permanent-magnet synchronous motor drive," *IEEE Trans. Ind. Appl.*, vol. IA-23, no. 4, pp. 681–689, Jul. 1987.

[2] M. Mengoni, L. Zarri, A. Tani, G. Serra, and D. Casadei, "A comparison of four robust control schemes for field-weakening operation of induction motors," *IEEE Trans. Power Electron.*, vol. 27, no. 1, pp. 307–320, Jan. 2012.

[3] Y. Liu, J. Zhao, and R. Wang, "Performance improvement of induction motor current controllers in field-weakening area for electric vehicles," *IEEE Trans. Power Electron.*, vol. 28, no. 5, pp. 2468–2482, May 2013.

[4] K. Sakai, T. Takahashi, E. Shimomura, M. Arata, Y. Nakazawa, and T. Tajima, "Development of permanent magnet reluctance motor suitable for variable-speed drive for electric vehicle," *IEEJ Trans. Ind. Appl.*, vol. 123-D, no. 6, pp. 681–688, Jun. 2004.

[5] V. Ostovic, "Memory motors," *IEEE Ind. Appl. Mag.*, vol. 9, no. 1, pp. 52–61, Jan./Feb. 2003.

[6] D. Ishak, Z. Q. Zhu, and D. Howe, "Permanent magnet brushless machines with unequal tooth widths and similar slot and pole numbers," in *Proc. IEEE/IAS Annu. Meeting*, 2004, vol. 2, pp. 1055–1061.

[7] P. Salminen, N. Niemela, J. Pyrhonen, and J. Mantere, "Performance analysis of fractional slot wound PM-motors for low speed applications," in *Proc. 39th IEEE/IAS Annu. Meeting*, 2004, vol. 2, pp. 1032–1037.

[8] A. M. E. L.-Refaie, T. M. Jahns, P. J. McCleer, and J. W. McKeever, "Experimental verification of optimal flux weakening in surface PM machines using concentrated windings," *IEEE Trans. Ind. Appl.*, vol. 42, no. 2, pp. 443–453, Mar. 2006.

[9] P. Salminen, N. Niemela, J. Pyrhonen, and J. Mantere, "High-torque low-torque-ripple fractional-slot PM-motors," in *Proc. IEEE Int. Conf. Electric Mach. Drives*, 2005, pp. 144–148.

[10] J. Cros and P. Viarouge, "Synthesis of high performance PM motors with concentrated windings," *IEEE Trans. Energy Convers.*, vol. 17, no. 2, pp. 725–727, Jun. 1999.

[11] H. Jussila, P. Salminen, N. Niemela, and J. Pyrhonen, "Guidelines for designing concentrated winding fractional slot permanent magnet machines," in *Proc. Int. Conf. Power Eng., Energy Electr. Drives*, 2007, pp. 191–194.

[12] N. A. Patil and J. S. Lawler, "Experimental verification of conventional phase advancement method for surface permanent magnet motor with fractional-slot concentrated windings," in *Proc. IEEE Southeastcon*, 2008, pp. 474–479.

[13] V. Ostovic, "Pole changing permanent magnet machines," *IEEE Trans. Ind. Appl.*, vol. 38, no. 6, pp. 1493–1499, Dec. 2002.

[14] K. Sakai, K. Yuki, Y. Hashiba, N. Takahashi, and K. Yasui, "Principle of the variable-magnetic-force memory motor," presented at the Int. Conf. Electr. Mach. Syst., Tokyo,, Japan, 2009, Paper LS6 A-1.

[15] K. Sakai, H. Hashimoto, and S. Kuramochi, "Principle and basic characteristics of hybrid variable-magnetic-force motors," in *Proc. 14th Eur. Conf. Power Electron. Appl.*, 2011, pp. 1–10.

[16] J. H. Lee and J. P. Hong, "Permanent magnet decreasing magnetization characteristics analysis of a variable flux memory motor using coupled Preisach modeling and FEM," *IEEE Trans. Magn.*, vol. 44, no. 6, pp. 1550–1553, Jun. 2008.

[17] H. C. Liu, H. Y. Lin, S. H. Fang, and Z. Q. Zhu, "Permanent magnet decreasing magnetization physics of a variable flux memory motor," *IEEE Trans. Magn.*, vol. 45, no. 10, pp. 4736–4739, Oct. 2009.

[18] I. Nitta, S. Maekawa, and T. Shiga, "Serial type variable-magnetic-force motor," in *Proc. Annu. Conf. IEEJ*, 2010, no. 5–13, pp. 20–21.

[19] S. Maekawa, K. Nagai, I. Nitta, and T. Hosoito, "Control method of variable magnetic force motor," in *Proc. Annu. Conf. IEEJ*, 2010, no. 5–11, pp. 17–18.

Sari Maekawa received the B.E. and M.E. degrees in electrical engineering from Hosei University, Tokyo, Japan, in 2001, and 2003, respectively.

In 2003, he joined Toshiba Corporation. He is with the Power and Industrial Systems R&D Center, Toshiba Corporation, Tokyo, Japan, and has been working on the development of Power electronics and Motor drives.

Mr. Maekawa is a Member of the Institute of Electrical Engineers of Japan.

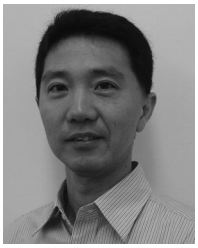

Kazuaki Yuki received the M.E. degree in electrical engineering from Keio University, Tokyo, Japan, in 1994.

In 1994, he joined Toshiba Corporation. He is with the Power and Industrial Systems R&D Center, Toshiba Corporation, Tokyo, Japan and has been working on the development of Drive system for railway.

Mr. Yuki is a Member of the Institute of Electrical Engineers of Japan.

Makoto Matsushita received the M.E. degree in electrical engineering from Tokyo University of Science, Chiba, Japan, in 1995.

In 1995, he joined Toshiba Corporation. He is with the Power and Industrial Systems R&D Center, Toshiba Corporation, Tokyo, Japan, and has been working on the development of motors.

Mr. Matsushita is a Member of the Institute of Electrical Engineers of Japan.

Isamu Nitta joined Toshiba Corporation, Yokohama, Japan in 1988, where he has been engaged in the Corporate Manufacturing Center. He has been working on the development of motors and magnetic applications.

Mr. Nitta is a Member of the Institute of Electrical Engineers of Japan.

Yukihisa Hasegawa received the B.E. and M.E. degrees in electrical engineering from Gifu University, Gifu, Japan, in 1988.

He joined Toshiba Corporation, Yokohama, Japan, in 1988, where he has been engaged in the Corporate Manufacturing Center. His special fields of interest include PM motor and motor control systems.

Mr. Hasegawa is a Member of the Institute of Electrical Engineers of Japan and The Japan Society for Precision Engineering.

Tsuyoshi Shiga joined Toshiba Home Appliances Corporation, Aichi, Japan, where he has been engaged in the Laundry Technology Department. He has been working on the development of Electronics of Laundry.

Tsuyoshi Hosoito received the B.E. degree in electrical engineering from Kanazawa Institute of Technology, Ishikawa, Japan, in 1984.

He joined Toshiba Home Appliances Corporation, Aichi, Japan in 1984, where he has been engaged in the Appliances Development Department. He has been working on the development of inverters and motors for Laundry.

Kazunobu Nagai received the B.E. degree in electrical engineering from Meiji University, Tokyo, Japan, in 1981.

He joined Toshiba Home Appliances Corporation, Aichi, Japan in 1981. He has been working on the development of inverters and motors for Laundry.

Hisao Kubota (M'87) received the B.E., M.E., and Ph.D. degrees in electrical engineering from Meiji University, Tokyo, Japan, in 1982, 1984, and 1989, respectively.

Since 1984, he has been a member of the faculty at Meiji University, where he is currently a Professor. His research interests include motor drives.

Dr. Kubota is a Member of the Institute of Electrical Engineers of Japan. He is also a member of the IEEE Power Electronics, Industry Applications, and Industrial Electronics Societies.